ACS APPLIED ENERGY MATERIALS

www.acsaem.org Article

Operando X-ray Absorption Spectroscopic Study on the Influence of Specific Adsorption of the Sulfo Group in the Perfluorosulfonic Acid Ionomer on the Oxygen Reduction Reaction Activity of the Pt/C Catalyst

Chen Liu, Tomoki Uchiyama,* Noriyuki Nagata, Masazumi Arao, Kentaro Yamamoto, Toshiki Watanabe, Xiao Gao, Hideto Imai, Syota Katayama, Seiho Sugawara, Kazuhiko Shinohara, Koichiro Oshima, Shigeki Sakurai, and Yoshiharu Uchimoto

Cite This: *ACS Appl. Energy Mater.* 2021, 4, 1143−1149 Read Online

ACCESS | Metrics & More | Article Recommendations | Supporting Information

ABSTRACT: The influence of specific adsorption of the sulfo group in the perfluorosulfonic acid ionomer, Nafion, on the oxygen reduction reaction (ORR) of a carbon-supported Pt/C catalyst using a thin-film rotating disk electrode was investigated. The relationship between the catalyst activity and coating of the Pt/C catalyst with Nafion was quantitatively evaluated through electrochemical measurements, *operando* X-ray absorption spectroscopy (XAS), and CO stripping voltammetry. Activity of the Pt/C catalyst decreased with increasing ionomer-to-carbon weight ratios. To date, the effect of specific adsorption on a catalyst has been investigated using CO stripping voltammetry. However, quantitative evaluation of specific adsorption at the ORR potential (0.50−1.0 V) has not been performed yet. We quantitatively evaluated the specific adsorption during the ORR by measuring the 5d orbital vacancy of the Pt/C catalyst using *operando* XAS. The difference in the electronic structures of Pt in the high potential range, with and without the ionomer, was successfully established.

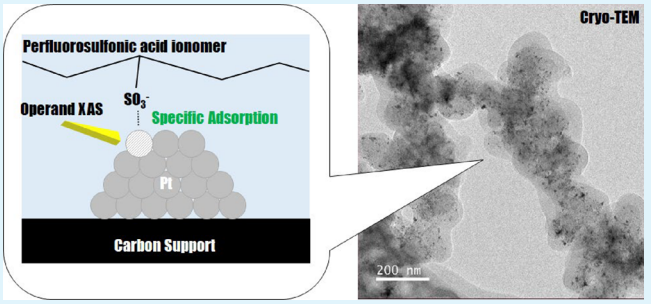

KEYWORDS: *fuel cells, Pt/C catalyst, oxygen reduction reaction activity, specific adsorption, ionomer, operando X-ray absorption spectroscopy*

INTRODUCTION

Polymer electrolyte fuel cells (PEFCs) are clean energy devices with polymer electrolytes and are expected to play an important role in the development of a global renewable energy system and a pure hydrogen energy society in the future. PEFCs have already been applied for small-scale energy systems such as fuel cell vehicles (FCVs).[1−5] However, several challenges must be overcome to realize the widespread use of FCVs. For successful commercialization, a reduction in the usage and cost of Pt cathode catalysts is necessary. Pt-based catalysts are basically used because of the relatively inefficient reaction kinetics and catalyst degradation under strong acidic conditions during the oxygen reduction reaction (ORR). However, there are still many difficulties in realizing acceptable cost-effective FCVs.[6,7] Therefore, a high ORR activity and reliable durability of the cathode catalyst layer are highly desirable for ensuring the widespread use of FCVs.

It is known that the ORR activity of Pt-based catalysts is reduced by specific adsorption of anionic species.[8] Perfluorosulfonic acid ionomers such as Nafion are commonly included in the catalyst layers of PEFCs to provide protonic pathways for promoting the ORR.[9,10] The loss in ORR activity of Nafion-capped Pt single crystals was found to follow the order Pt (111) > (110) > (100). This trend is same as that on Nafion-free surfaces in a sulfuric acid solution.[11] Polycrystalline Pt and Pt alloy surfaces also show loss in activity when capped with Nafion.[8] These reports suggested that the adsorption of a sulfo group anion from the side chain of Nafion blocked the active site of Pt.[12] A similar behavior has been observed for Pt-based catalysts (Pt/C), but the extent of decrease in the ORR activity varies depending on the carbon structure.[13−18] The properties of the carbon support are crucial in reducing the poisoning effect of perfluorosulfonic acid ionomers and in improving the catalyst performance.[16−18] Catalysts prepared from porous carbons with 4−7 nm opening pores show

Received: September 20, 2020
Accepted: January 6, 2021
Published: January 21, 2021

https://dx.doi.org/10.1021/acsaem.0c02326
ACS Appl. Energy Mater. 2021, 4, 1143−1149

excellent ORR activities and transport properties.[18] Shinozaki et al. studied the impact of Nafion on the ORR activities of Pt/C and Pt-alloy/C catalysts using a rotating disk electrode (RDE) and found that catalysts with a high surface area of carbon could mitigate the loss in activity because Pt nanoparticles located inside the pores of the high-surface-area carbon inhibited the ionomer coverage.[19] These studies clearly indicate that quantification of the ionomer coverage is important for designing new catalysts.

An electrochemical method is an alternative method for estimating the ionomer coverage on Pt surfaces. In the CO displacement method, a constant potential was applied while introducing the CO gas.[11,20−23] When CO displaced the adsorbing species on Pt, oxidation or reduction currents were generated depending on the displaced species, and the ionomer coverage was estimated based on this.[11] Using this method, Takeshita et al. quantitatively determined the ionomer coverage and found that the ionomer coverage of a Pt catalyst on a porous carbon support was lower than that on a nonporous catalyst.[24] While the CO displacement method is useful for determining the ionomer coverage, the potential range during measurement is limited, which is a drawback. Because the adsorbed CO molecules on the Pt surface is oxidized at ∼0.6 V vs RHE (reversible hydrogen electrode), the potential range of only 0.08−0.56 V vs RHE could be used to evaluate the anion adsorption.[11,20−23,25]

To observe the anion adsorption on Pt, spectroscopic methods such as X-ray absorption spectroscopy (XAS) for single crystal Pt(111) electrode surfaces in H_2SO_4 solution have been developed.[26−28] Combining X-ray absorption near edge structure (XANES) and full-multiple scattering calculations using the FEFF8 code, it was concluded that specific anion adsorption occurred significantly in 1 M H_2SO_4 but did not occur in 1 M $HClO_4$.[26] However, direct observation of anion adsorption on practical Pt nanoparticle/C catalysts for perfluorosulfonic acid ionomers using XAS has been reported less so far. In this paper, to achieve specific adsorption observation over a higher potential range that is at least equal to the ORR active potential (around 0.90 V vs RHE), which cannot be measured by the CO displacement method, *operando* XAS measurements were performed; the electronic status and local structural change of Pt atoms induced by the specific adsorption of anions at any potential were observed. *Operando* XAS measurement is a reliable method for observing the electronic status, detailed structure of the Pt surface,[29,30] and the strain-inducing compression/extension of the Pt−Pt bond length.[31] Here, we report *operando* fluorescence XAS measurements to directly obtain the signal from the catalyst loaded on RDE with the exact same amount of loading as in the electrochemical measurement to ensure accurate XAS spectra and ORR activity.

In this study, we evaluated the ORR activities of commercial Pt/C catalysts with various ionomer-to-carbon (I/C) weight ratios (0.0, 0.20, 0.50, and 1.0). The morphology of the Pt/C catalyst covered with swollen ionomers was investigated by cryo-transmission electron microscopy (cryo-TEM). CO stripping voltammetry measurements, *operando* X-ray absorption fine structure analysis, and analysis of 5d orbital vacancy were used to quantitatively assess the anion adsorption among Pt/C catalysts with various I/C ratios. The various adsorption species on the Pt surface in the low (0.02−0.50 V vs RHE) and high (0.50−1.0 V vs RHE) potential ranges have been discussed.

EXPERIMENTAL METHODS

Electrochemical Measurements. The Pt/C (29.1 wt %; TEC10V30E, average particle size of 3 nm, observed by TEM) catalyst supported was purchased from TKK Co. Ltd., Japan. The Pt/C catalyst ink contained water and 2-propanal in a 3:2 ratio (99.99%, FUJIFILM Wako Pure Chemical Corporation, Japan), and the amount of Pt/C was adjusted to form a 20 μg_{carbon} cm^{-2} catalyst layer after dropping 10 μL on a glassy carbon RDE (GC RDE, HOKUTO DENKO, Japan; 0.196 cm^2 area). The ink on the RDE was dried at 700 rpm at room temperature. Nafion solution (5 wt %, Sigma-Aldrich Co. LLC, Japan) was employed to prepare Pt/C catalyst ink with I/C ranging from 0.0 to 1.0. The high-purity $HClO_4$ (Kanto Chemical Co., Inc., Japan, purity: 60.0 wt %) was adopted to prepare the 0.1 M $HClO_4$ electrolyte. The water used for preparing the electrolyte was from ultrapure water with electrical resistivity of 18.2 MΩ·cm or more (Milli-Q, Millipore A/S).

ORR activity measurements were carried out in a three-electrode cell at 25 °C. The counter electrode was a Pt mesh, and the reference electrode was RHE. Prior to catalyst activity measurements, the potential was cycled 50 times between 0.02 and 1.0 V (vs RHE) at 200 mVs^{-1} to obtain a stable cyclic voltammogram in N_2-saturated 0.1 M $HClO_4$. The final CV was obtained at 50 mVs^{-1}. After the cyclic voltammetry (CV) measurements, the electrolyte was saturated with O_2. Then, hydrodynamic voltammograms were obtained between 0.2 and 1.2 V vs RHE at 10 mVs^{-1} from 100 to 2500 rpm. The oxygen reduction data for all the catalysts were analyzed according to Koutechy-Levich equation. The oxygen coverage was measured by linear sweep voltammetry in N_2-saturated 0.1 M $HClO_4$. The potential was swept from 0.40 V (vs RHE) to the target potential (0.50−1.0 V vs RHE) at 50 mVs^{-1} and then the potential was held for 5 min to obtain a stable current. At last, the potential was swept to 0.40 V (vs RHE). The oxygen coverage was calculated through the oxide reduction charge to hydrogen adsorption charge.[32] The integrated cathodic current was used to estimate the charge of oxide species based on the following reaction, ($Pt\text{-}OH + H^+ + e^- \rightarrow Pt + H_2O$), and also reports from another researcher.[32]

CO stripping voltammetry measurements were conducted in the same three-electrode cell at 25 °C. The potential was cycled 50 times between 0.02 and 1.0 V (vs RHE) at 200 mVs^{-1}. The final cyclic voltammogram was obtained with 50 mVs^{-1}. Then, the potential was held at 0.12−0.5 V (vs RHE), with N_2 bubbling for 10 min until a stable current was obtained. After that, the gas was immediately switched to CO (99.9%, GL Sciences Inc.) for about 20 s to obtain a stable current, indicating complete CO adsorption. The bubbling gas was switched again to N_2 for 40 min for CO deaeration. Finally, CO stripping voltammetry was initiated in the range of 0.02 to 1.0 V (vs RHE). The coverage of anions was estimated through 2 times of total CO displacement current divided by CO stripping charge.

TEM Observations. The specimens for TEM observation were prepared by drying sample inks on a Cu grid. For I/C = 0.10, 0.20, 0.50, and 1.0 samples, specimens were kept at 60 °C and 80% of relative humidity for 5 min and then quickly frozen with liquid ethane using an EM GP2 plunge freezer (Leica Microsystems, Austria). The frozen specimens were studied using TEM in liquid nitrogen by using a cryo-transfer holder. Cryo-TEM observation was carried out at about −175 °C on a JEM-F200 (JEOL Ltd., Japan) microscope operating at 200 kV. For the I/C = 0.0 sample, the conventional TEM observation was carried out on a JEM-F200 (JEOL Ltd., Japan) microscope operating at 200 kV. During cryo-TEM observation, we observed the ionomer suffer the damage from the electron beam, as shown in Figure S1. Therefore, the observation was conducted in short exposure time.

***Operando* XAS Measurements.** *Operando* XAS measurements for Pt L_{III}-edge of Pt/C catalysts were carried out in fluorescence mode using synchrotron radiation at BL37XU of SPring-8, Hyogo, Japan. A pair of Si (111) monochromators and a total-reflection Rh mirror (4 mrad) were used to obtain collimated and monochromatic X-rays. Prior to the experiments, the samples were electrochemically cleaned by CV in the range 0.0−1.1 V (vs RHE). The electrode

https://dx.doi.org/10.1021/acsaem.0c02326
ACS Appl. Energy Mater. 2021, 4, 1143−1149

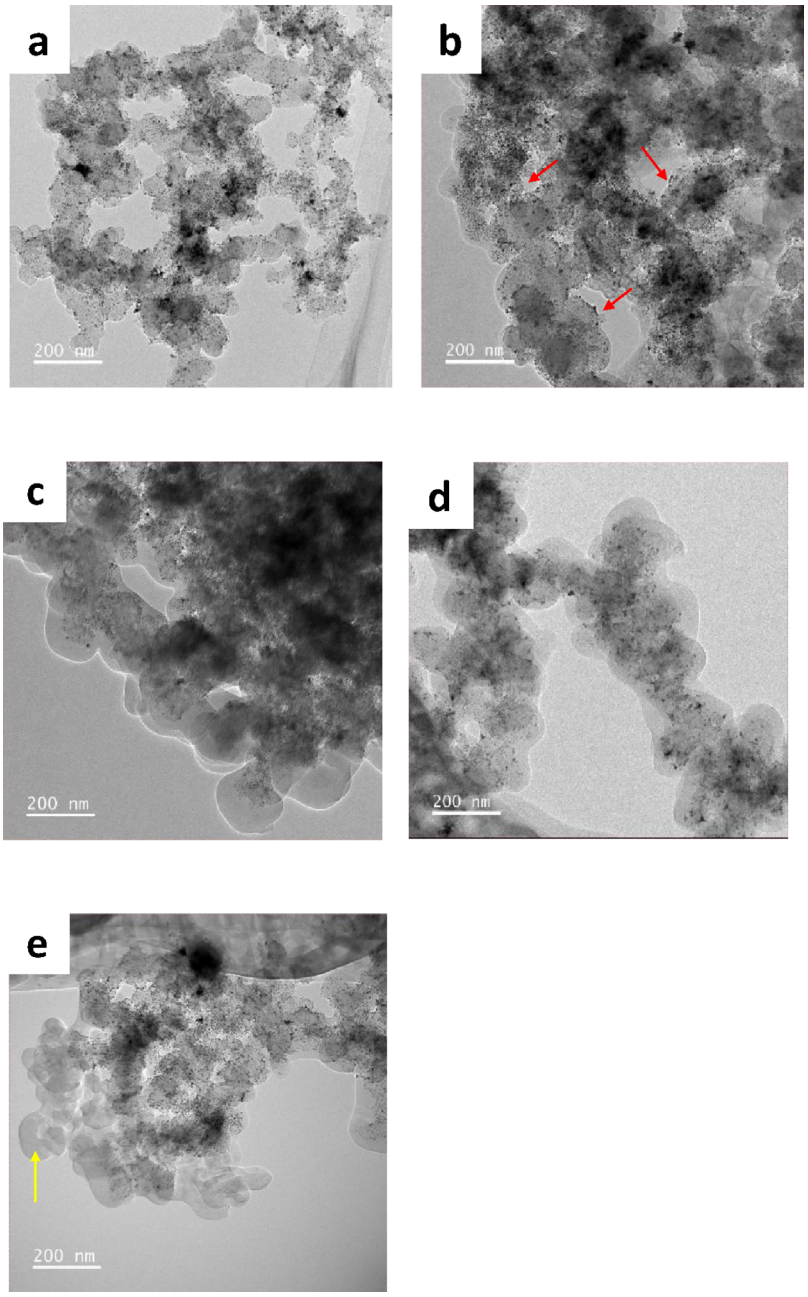

Figure 1. Transmission electron microscopy (TEM) images of the Pt/C catalyst at various I/C ratios. I/C = (a) 0.0, (b) 0.10, (c) 0.20, (d) 0.50, and (e) 1.0. Red arrows in (b) indicate the exposed surface of the catalyst. The yellow arrow in (e) shows the isolated ionomer.

potential was swept cathodically from 0.5 to 1.1 V (vs RHE). Data were analyzed using ATHENA and ARTEMIS, a suite of the IFEFFIT software programs.[33]

RESULTS AND DISCUSSIONS

TEM Observations. Pt/C nanoparticles with various I/C ratio ink were observed by cryo-TEM, as shown in Figure 1. Figure 1a shows the TEM image of a Pt/C catalyst without an ionomer (I/C = 0.0), showing typical morphologies of a carbon-supported Pt catalyst. In I/C = 0.10, the Pt/C catalyst surface was partly exposed, as indicated by the arrows in Figure 1b, and the observed thickness of the ionomer covering the catalyst was smaller than the samples of I/C = 0.20, 0.50, and 1.0. Judging from the TEM images, the catalyst particles were fully covered by the ionomer in I/C = 0.20 (Figure 1c). When the I/C was over 0.20, all the Pt/C catalysts were surrounded by ionomers, as shown in Figure 1c–e. In addition, some isolated ionomer was found in I/C = 1.0, as indicated by the arrow in Figure 1e. The carbon aggregate and morphology of ionomers observed in this study has a good agreement with a previous report.[34]

Electrochemical Measurements. Figure 2 shows the cyclic voltammograms of the Pt/C catalyst ink with I/C ratios from 0.0 to 1.0, and the increase of hydrogen under potential deposition (UPD) and the oxide formation region are shown in Figure S2. No significant change in the voltammograms between 0.0 and 1.0 V (vs RHE) was observed with a changing I/C ratio. There was a slight onset potential shift with the increasing I/C ratio from 0.0 to 1.0 and a negative shift in the onset of hydrogen underpotential deposition current and slight

https://dx.doi.org/10.1021/acsaem.0c02326
ACS Appl. Energy Mater. 2021, 4, 1143–1149

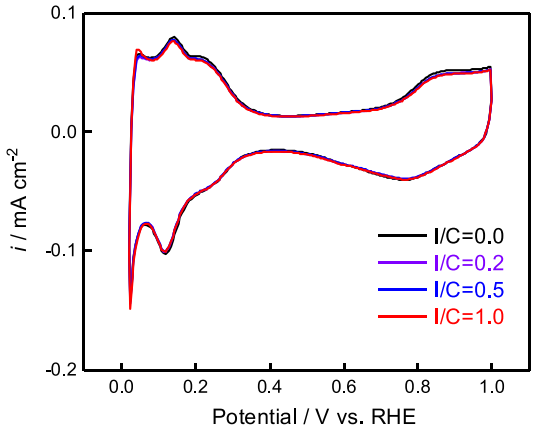

Figure 2. Cyclic voltammogram for Pt/C with varying I/C ratios.

shifts on the onset potential of oxide formation (Figure S2a,b). This tendency was identical to the results reported by Shinozaki et al.,[19] who used the low surface area carbon-supported Pt catalyst as we are using Vulcan as a carbon support. Other researchers, Zhu et al., reported on the effect of specific adsorption of Nafion's sulfo groups.[35] They also evaluated the CV curves of the Pt/C catalyst (TEC10E50E, TKK) with an I/C ratio from 0 to 1.33. Their CV result using high surface area carbon-supported Pt shows a slight positive shift of onset potential of Pt oxidation. Even with the same type of carbon support, the cyclic voltammogram reported by Zhu et al. is less clear in the effect of the Nafion coating than the one reported by Shinozaki et al.

Although the effect of ionomer content on the Pt/C catalyst could be not clearly observed through CV measurements, we found that the catalyst activity, including specific activity, changed with varying I/C ratios. To illustrate the effect of ionomers on the catalyst activity at 0.90 V (vs RHE) for various ionomer contents, the specific activity and electrochemical surface area (ECSA) were plotted against the I/C ratio, as shown in Figure 3, and the linear sweep voltammogram and Koutecky–Levich plot are shown in Figures S3–S7. The Pt/C catalyst had the highest specific activity at I/C = 0.0 (ionomer-free), and we could observe that the diffusion limit current is larger at the low I/C ratio, as shown in Figure S8, suggesting a slight oxygen diffusion resistance in the high I/C ratio. The catalyst activity began to decrease with the increasing ionomer content, but the ECSA remained almost the same as that for the ionomer-free system. These results were consistent with those of a previous study[36] and indicate that the ionomer decreases Pt/C catalyst activity, but at the same time, does not affect the ECSA. It was clear that the limiting current did not change in I/C < 0.20, and the ORR activity decreased, as shown in Figure S8. This phenomenon indicates that the decreasing activity is not caused by the oxygen concentration effect. From I/C = 0.50–1.0, the limiting current was changed from that of I/C = 0.0–0.20, but as the ORR activity was estimated at charge transfer rate-determining potential (0.90 V vs RHE), the oxygen concentration did not have a significant effect on the activity. The report from Zhu et al. indicates that the linear sweep voltammogram of the Pt/C catalyst with I/C from 0.0 to 1.33 has also been evaluated.[35] They indicated that the limiting current density in the mass control region slightly decreased upon the increasing I/C ratio, while the activity has no noticeable difference at the same time, which is in agreement with our results. Here, we conjecture that the increased specific adsorption of the Pt/C catalyst contributed to the activity loss due to the higher ionomer content (higher I/C ratios).

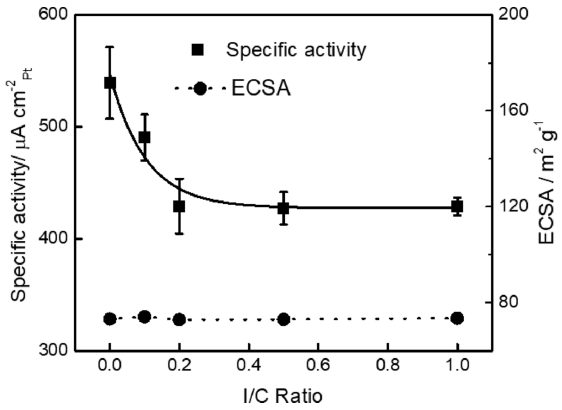

Figure 3. Influence of the I/C ratio on the ECSA and specific activity of Pt/C at 0.90 V vs RHE.

To clarify the specific adsorption effect of the ionomer at a high potential range (0.70–0.90 V vs RHE), we first need to evaluate the oxygen coverage. The oxide reduction profiles for Pt/C catalysts with I/C = 1.0 are shown in Figure S9 as an example. The oxygen coverage increased at higher potentials for all the I/C ratios (Figure 4); at the same time, the adsorption of oxide species increased, which is in agreement with previously reported results.[37] The oxygen coverage in the Pt/C catalyst was slightly increased in I/C = 0.0, which agrees with the CV results described in Figure S2. This indicates that oxygen coverage does not mainly contribute to the change in the Pt/C catalyst activity when the I/C ratios are varied from 0.0 to 1.0. Here, we can reasonably speculate that the Pt/C catalyst activity decreases with the increasing I/C ratio and is mainly affected by the specific adsorption species from the ionomer.

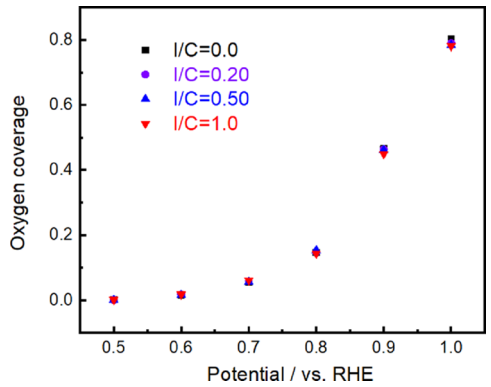

Figure 4. Dependence of the I/C ratio on the oxygen coverage for Pt/C.

To quantitatively evaluate the specific adsorption species, we used CO stripping voltammetry, which measures the displacement charge from the adsorption species to CO. The charge during each exchange reaction, Pt-H at 0.12 V (vs RHE), and the anion adsorption species on Pt at 0.40 V (vs RHE) or more were calculated, as shown in Figure 5. The examples of CO exchange current profiles are shown in Figure S10. At 0.12 V

https://dx.doi.org/10.1021/acsaem.0c02326
ACS Appl. Energy Mater. 2021, 4, 1143–1149

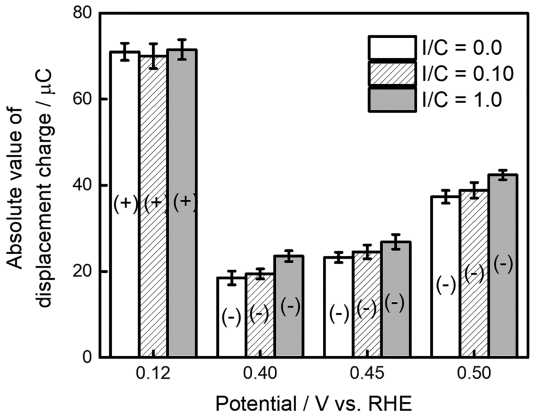

Figure 5. CO displacement charge measurements as a function of measurement potential for Pt/C with I/C = 0.0, 0.10, and 1.0. (+)/(−) indicates the polarity of the CO displacement charge.

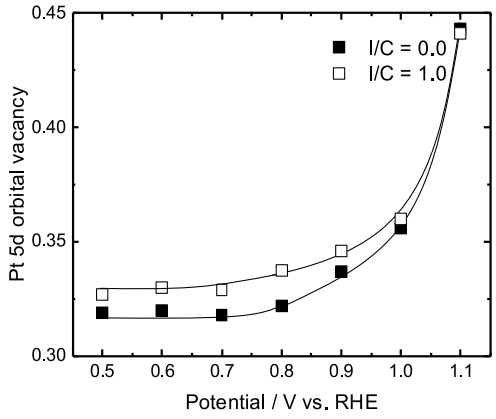

Figure 6. Change in 5d orbital vacancy of Pt/C catalysts with I/C = 0.0 and 1.0 from 0.5 to 1.1 V.

(vs RHE), the hydrogen adsorbed species show no obvious change, similar to that observed for the ECSA. In the potential range 0.40−0.50 V (vs RHE), the CO displacement charge of the Pt/C catalyst with I/C = 1.0 was obviously higher than that of the ionomer-free sample at each potential, which is in agreement with the previous reports on ionomer- or anion-specific adsorption through CO displacement measurement.[32,38,39] I/C = 0.10 showed the displacement charge between I/C = 0.0 and 1.0 from 0.40 to 0.50 V (vs RHE). This result using I/C = 0.10 was consistent with the results obtained from the cryo-TEM image as well as the specific activity. This result confirmed that the ionomer coverage impacts the CO displacement charge. For the anion coverage based on the CO exchange current, we calculated the anion coverage by 2*(CO displacement charge)/(CO stripping charge), and the CO stripping profile and the results are shown in Figures S11 and S12, respectively. In comparison, the report by Garrick et al.[38] reported the anion coverage of the Pt/C catalyst in the presence and absence of H_2SO_4. The anion coverage of Pt/C in the presence and absence of H_2SO_4 was 0.25/0.15 at 0.50 V (vs RHE), which was consistent with our report on I/C = 0.0 and 1.0. These indicate that the amount of specific adsorption increases with the increasing ionomer content. All the above observations lead to the conclusion that the increasing amount of adsorption species in the ionomer-containing group is attributable to ionomer-specific adsorption, and this is suggested to be the primary reason for the decreasing Pt/C catalyst activity with increasing ionomer contents.

***Operando* XAS Measurements.** Although ionomer adsorption may be one of the main reasons for the lower catalyst activity, as revealed by the CO displacement measurement, only the adsorption species at voltages lower than 0.60 V (vs RHE) could be analyzed. To observe the adsorption species in the high potential region, where the ORR occurred, *operando* XAS measurements were conducted, as shown in Figure S13−15. In this study, the number of 5d orbital vacancies in Pt was calculated from the XANES spectra of Pt L_{III}-edge and L_{II}-edge[39] (Figure S16), and the chemical state (oxidation state) of Pt was determined. The detailed calculation method is described in the Supporting Information. The 5d orbital vacancies in the Pt/C catalyst with I/C = 0.0 and 1.0 are shown in Figure 6. The calculation of 5d orbital vacancies was based on the report by Mansour et al.,[40] and the brief illustration of the procedure is shown Figure S17.

The 5d orbital vacancies increase with increasing potential for all the samples, suggesting an increased Pt−O bond formation. This trend is similar to that discussed above. By comparing the 5d orbital vacancies of the Pt/C catalysts with I/C = 0.0 and 1.0, it can be easily determined that the 5d orbital vacancies of the catalyst with I/C = 1.0 are more than those of the Nafion-free sample at 0.90 V (vs RHE), where the ORR occurs. Although the sulfo group is a monobasic acid and cannot always be compared to the dibasic acid, these trends are consistent with previously reported results comparing $HClO_4$ and H_2SO_4 solution.[20] There is significant evidence that the ionomer is involved in more specific adsorption on the Pt/C catalyst, changes the electric state of Pt atoms, and increases the 5d orbital vacancies. Because we have already found that the Pt-O species or oxygen coverage did not change in the high potential region (0.50−1.0 V vs RHE), the change in the electronic state of Pt atoms should be caused by the extra specific adsorption species from the ionomer coverage. Through this measurement technique, we have developed a new method to quantitatively investigate the specific adsorption through *operando* X-ray absorption fine structure analysis and 5d orbital vacancies in the high potential range, where the ORR occurs (0.70−0.90 V vs RHE). For comparison with the results reported by Teliska et al.,[26] the delta-mu spectra was obtained by $\Delta\mu = \mu$(X V vs RHE) − μ(0.50 V vs RHE), where μ(X V vs RHE) indicates the XANES spectra obtained at X = 0.60−1.1 V (vs RHE). When it was compared with their results (Figure S18), the behavior of I/C = 1.0 along with the potential in terms of the peak at 9 eV was similar to that reported by Teliska et al., indicating that the specific adsorption of the sulfo group also occurs in our study. In addition, the behavior of I/C = 0.0 along with the potential was also similar to that reported by Teliska et al. In particular, the peak that appeared at 8 eV (1.0 V vs RHE) was lower than that of I/C = 1.0 and showed a slight positive shift at 1.1 V vs RHE. According to these results, the specific adsorption of the sulfo group in I/C = 0.0 and 1.0 can be observed from XANES and is consistent with previous reports by Teliska et al. under $HClO_4$ and H_2SO_4 solutions, respectively. These results indicate that in the high potential range, the Pt/C catalyst activity decreases with increasing ionomer content and specific adsorption species.

https://dx.doi.org/10.1021/acsaem.0c02326
ACS Appl. Energy Mater. 2021, 4, 1143−1149

CONCLUSIONS

In this study, the impact of ionomers on the ORR of a carbon-supported Pt/C catalyst using a thin-film RDE in 0.1 M $HClO_4$ was investigated. The specific activity decreased as the I/C ratio increased from 0.0 to 0.20. We utilized many methods to evaluate the adsorption species separately, including the measurements of ECSA and oxygen coverage, CO stripping voltammetry, *operando* X-ray absorption fine structure, and analysis of 5d orbital vacancy. The ECSA and oxygen coverage did not change with the increasing ionomer content, indicating that the Pt/C catalyst activity was affected by other adsorption species. Comparison of the CO displacement charge and 5d orbital vacancies of the Pt/C catalysts with I/C = 0.0 and 1.0 suggests that the ionomer-specific adsorption increases when the I/C ratio of the Pt/C catalyst is 1.0; active sites on the surface of the Pt/C catalyst are occupied, resulting in a lower catalyst activity.

ASSOCIATED CONTENT

Supporting Information

The Supporting Information is available free of charge at https://pubs.acs.org/doi/10.1021/acsaem.0c02326.

Cryo-TEM image, I/C dependence of cyclic voltammogram, Liner sweep voltammograms and Koutecky–Levich plots, reduction current profiles, current-time response, CO stripping voltammogram, anion coverage of for Pt/C catalyst, measurement schematics for *operando* XAS measurement, structure of electrochemical cell for *operando* XAS measurement, XANES spectra, and a brief illustration for calculating the 5d orbital vacancy (PDF)

AUTHOR INFORMATION

Corresponding Author

Tomoki Uchiyama − *Graduate School of Human and Environmental Studies, Kyoto University, Kyoto 606-8501, Japan*; orcid.org/0000-0003-4880-7498; Email: uchiyama.tomoki.3x@kyoto-u.ac.jp

Authors

Chen Liu − *Graduate School of Human and Environmental Studies and Graduate School of Advanced Integrated Studies in Human Survivability (Shishu-Kan), Kyoto University, Kyoto 606-8501, Japan*

Noriyuki Nagata − *Graduate School of Human and Environmental Studies, Kyoto University, Kyoto 606-8501, Japan*

Masazumi Arao − *Analysis Platform Development Department, NISSAN ARC, LTD, Yokosuka, Kanagawa 237-0061, Japan*

Kentaro Yamamoto − *Graduate School of Human and Environmental Studies, Kyoto University, Kyoto 606-8501, Japan*; orcid.org/0000-0002-8739-4246

Toshiki Watanabe − *Graduate School of Human and Environmental Studies, Kyoto University, Kyoto 606-8501, Japan*

Xiao Gao − *Graduate School of Human and Environmental Studies, Kyoto University, Kyoto 606-8501, Japan*

Hideto Imai − *Analysis Platform Development Department, NISSAN ARC, LTD, Yokosuka, Kanagawa 237-0061, Japan*; orcid.org/0000-0002-9434-1492

Syota Katayama − *Fuel Cell Cutting-Edge Research Center Technology Research Association (FC-Cubic), Tokyo 135-0064, Japan*

Seiho Sugawara − *Fuel Cell Cutting-Edge Research Center Technology Research Association (FC-Cubic), Tokyo 135-0064, Japan*

Kazuhiko Shinohara − *Fuel Cell Cutting-Edge Research Center Technology Research Association (FC-Cubic), Tokyo 135-0064, Japan*

Koichiro Oshima − *Graduate School of Advanced Integrated Studies in Human Survivability (Shishu-Kan), Kyoto University, Kyoto 606-8306, Japan*

Shigeki Sakurai − *Graduate School of Advanced Integrated Studies in Human Survivability (Shishu-Kan), Kyoto University, Kyoto 606-8306, Japan*

Yoshiharu Uchimoto − *Graduate School of Human and Environmental Studies, Kyoto University, Kyoto 606-8501, Japan*; orcid.org/0000-0002-1491-2647

Complete contact information is available at: https://pubs.acs.org/10.1021/acsaem.0c02326

Notes

The authors declare no competing financial interest.

ACKNOWLEDGMENTS

The synchrotron radiation experiments were performed at the BL37XU, BL01B1, BL19B2, BL14B2 beamline of SPring-8 with the approval of the Japan Synchrotron Radiation Research Institute (JASRI) (Proposal No.2018A1037, 2018A1750, 2018B1616, 2018A1019, 2019B1899, 2020A1801, 2020A1799, 2020A1800). This work is based on results obtained from a project (JPNP20003) commissioned by the New Energy and Industrial Technology Development Organization (NEDO) of Japan.

REFERENCES

(1) Hamada, Y.; Nakamura, M.; Kubota, H.; Ochifuji, K.; Murase, M.; Goto, R. Field performance of a polymer electrolyte fuel cell for a residential energy system. *Renew. Sustainable Energy Rev.* **2005**, *9*, 345−362.

(2) Hamada, Y.; Goto, R.; Nakamura, M.; Kubota, H.; Ochifuji, K. Operating Results and Simulations on a Fuel cell for Residential Energy Systems. *Energy Convers. Manag.* **2006**, *47*, 3562−3571.

(3) Hamada, Y.; Takeda, K.; Goto, R.; Kubota, H. Hybrid utilization of renewable energy and fuel cells for residential energy systems. *Energy Buildings* **2011**, *43*, 3680−3684.

(4) Iain, S.; Daniel, S.; Anthony, V. A.; Paul, B.; Paul, E. D.; Paul, E.; Nilay, S.; Kate, R. W. The role of hydrogen and fuel cells in the global energy system. *Energy Environ. Sci.* **2019**, *12*, 463−491.

(5) Dupuis, A. C. Proton exchange membranes for fuel cells operated at medium temperatures: Materials and experimental techniques. *Prog. Mater. Sci.* **2011**, *56*, 289−327.

(6) Sundmacher, K. Fuel Cell Engineering: Toward the Design of Efficient Electrochemical Power Plants. *Ind. Eng. Chem. Res.* **2010**, *49*, 10159−10182.

(7) Rabis, A.; Rodriguez, P.; Schmidt, T. J. Electrocatalysis for Polymer Electrolyte Fuel Cells: Recent Achievements and Future Challenges. *ACS Catal.* **2012**, *2*, 864−890.

(8) Subbaraman, R.; Strmcnik, D.; Paulikas, A. P.; Stamenkovic, V. R.; Markovic, N. M. Oxygen reduction reaction at three-phase interfaces. *J. Chem. Phys. Phys. Chem.* **2010**, *11*, 2825−2833.

(9) Pivovar, A. M.; Pivovar, B. S. Dynamic Behavior of Water within a Polymer Electrolyte Fuel Cell Membrane at Low Hydration Levels. *J. Phys. Chem. B* **2005**, *109*, 785−793.

(10) Kusoglu, A.; Weber, A. Z. New Insights into Perfluorinated Sulfonic-Acid Ionomers. *Chem. Rev.* **2017**, *117*, 987−1104.
(11) Subbaraman, R.; Strmcnik, D.; Stamenkovic, V.; Markovic, N. M. Three Phase Interfaces at Electrified Metal-Solid Electrolyte Systems 1. Study of the Pt(Hkl)-Nafion Interface. *J. Phys. Chem. C* **2010**, *114*, 8414−8422.
(12) Owejan, J. P.; Owejan, J. E.; Gu, W. Impact of Platinum Loading and Catalyst Layer Structure on PEMFC Performance. *J. Electrochem. Soc.* **2013**, *160*, F824−F833.
(13) Higuchi, E.; Uchida, H.; Watanabe, M. Effect of loading level in platinum-dispersed carbon black electrocatalysts on oxygen reduction activity evaluated by rotating disk electrode. *J. Electroanal. Chem.* **2005**, *583*, 69−76.
(14) Curnick, O. J.; Pollet, B. G.; Mendes, P. M. Nafion-stabilised Pt/C electrocatalysts with efficient catalyst layer ionomer distribution for proton exchange membrane fuel cells. *RSC Adv.* **2012**, *2*, 8368−8374.
(15) Speder, J.; Altmann, L.; Roefzaad, M.; Bäumer, M.; Kirkensgaard, J. J. K.; Mortensen, K.; Arenz, M. Pt based PEMFC catalysts prepared from colloidal particle suspensions−a toolbox for model studies. *Phys. Chem. Chem. Phys.* **2013**, *15*, 3602−3608.
(16) Kamitaka, Y.; Takeshita, T.; Morimoto, Y. MgO-Templated Mesoporous Carbon as a Catalyst Support for Polymer Electrolyte Fuel Cells. *Catalysts* **2018**, *8*, 230.
(17) Ramaswamy, N.; Gu, W.; Ziegelbauer, J. M.; Kumaraguru, S. Carbon Support Microstructure Impact on High Current Density Transport Resistances in PEMFC Cathode. *J. Electrochem. Soc.* **2020**, *167*, No. 064515.
(18) Yarlagadda, V.; Carpenter, M. K.; Moylan, T. E.; Kukreja, R. S.; Koestner, R.; Gu, W.; Thompson, L.; Kongkanand, A. Boosting Fuel Cell Performance with Accessible Carbon Mesopores. *ACS Energy Lett.* **2018**, *3*, 618−621.
(19) Shinozaki, K.; Morimoto, Y.; Pivovar, B. S.; Kocha, S. S. Suppression of oxygen reduction reaction activity on Pt-based electrocatalysts from ionomer incorporation. *J. Power Sources* **2016**, *325*, 745−751.
(20) Clavilier, J.; Albalat, R.; Gomez, R.; Orts, J. M.; Feliu, J. M.; Aldaz, A. Study of the charge displacement at constant potential during CO adsorption on Pt(110) and Pt(111) electrodes in contact with a perchloric acid solution. *J. Electroanal. Chem.* **1992**, *330*, 489−497.
(21) Orts, J. M.; Fernández-Vega, A.; Feliu, J. M.; Aldaz, A.; Clavilier, J. Electrochemical behaviour of CO layers formed by solution dosing at open circuit on Pt(111). Voltammetric determination of CO coverages at full hydrogen adsorption blocking in various acid media. *J. Electroanal. Chem.* **1992**, *327*, 261−278.
(22) Clavilier, J.; Albalat, R.; Gómez, R.; Orts, J. M.; Feliu, J. M. Displacement of adsorbed iodine on platinum single-crystal electrodes by irreversible adsorption of CO at controlled potential. *J. Electroanal. Chem.* **1993**, *360*, 325−335.
(23) Feliu, J. M.; Orts, J. M.; Gómez, R.; Aldaz, A.; Clavilier, J. New information on the unusual adsorption states of Pt(111) in sulphuric acid solutions from potentiostatic adsorbate replacement by CO. *J. Electroanal. Chem.* **1994**, *372*, 265−268.
(24) Takeshita, T.; Kamitaka, Y.; Shinozaki, K.; Kodama, K.; Morimot, Y. Evaluation of ionomer coverage on Pt catalysts in polymer electrolyte membrane fuel cells by CO stripping voltammetry and its effect on oxygen reduction reaction activity. *J. Electroanal. Chem.* **2020**, *871*, 114250.
(25) Jomori, S.; Nonoyama, N.; Yoshida, T. Analysis and modeling of PEMFC degradation: Effect on oxygen transport. *J. Power Sources* **2012**, *215*, 18−27.
(26) Teliska, M.; Murthi, V. S.; Mukerjee, S.; Ramaker, D. E. Site-Specific vs Specific Adsorption of Anions on Pt and Pt-Based Alloys. *J. Phys. Chem. C* **2007**, *111*, 9267−9274.
(27) Teliska, M.; O'Grady, W. E.; Ramaker, D. E. Determination of H Adsorption Sites on Pt/C Electrodes in HClO4 from Pt L23 X-ray Absorption Spectroscopy. *J. Phys. Chem. B* **2004**, *108*, 2333−2344.
(28) Teliska, M.; O'Grady, W. E.; Ramaker, D. E. Determination of O and OH Adsorption Sites and Coverage in Situ on Pt Electrodes from Pt L23 X-ray Absorption Spectroscopy. *J. Phys. Chem. B* **2005**, *109*, 8076−8084.
(29) Liang, Z.; Song, L.; Deng, S.; Zhu, Y.; Stavitski, E.; Adzic, R. R.; Chen, J.; Wang, J. X. Direct 12-Electron Oxidation of Ethanol on a Ternary Au (core)-PtIr (shell) Electrocatalyst. *J. Am. Chem. Soc.* **2019**, *141*, 9629−9636.
(30) Sasaki, K.; Kuttiyiel, K. A.; Adzic, R. R. Designing high performance Pt monolayer core−shell electrocatalysts for fuel cells. *Curr. Opin. Electrochem.* **2020**, *21*, 368−375.
(31) Wang, X.; Orikasa, Y.; Takesue, Y.; Inoue, H.; Nakamura, M.; Taketoshi, M.; Nagahiro, H.; Uchimoto, Y. Quantitating the Lattice Strain Dependence of Monolayer Pt Shell Activity toward Oxygen Reduction. *J. Am. Chem. Soc.* **2013**, *135*, 5938−5941.
(32) Sugawara, S.; Tsujita, K.; Mitsushima, S.; Shinohara, K.; Ota, K. Simultaneous Electrochemical Measurement of Oxygen Reduction and Pt Oxide Formation/Reduction on Pt Nanoparticle Surface. *Electrocatal* **2011**, *2*, 60−68.
(33) Rehr, J. J.; Albers, R. C. Theoretical approaches to x-ray absorption fine structure. *Rev. Mod. Phys.* **2000**, *72*, 621.
(34) Takahashi, S.; Shimanuki, J.; Mashio, T.; Ohma, A.; Tohma, H.; Ishihara, A.; Ito, Y.; Nishino, Y.; Miyazawa, A. Observation of ionomer in catalyst ink of polymer electrolyte fuel cell using cryogenic transmission electron microscopy. *Electrochim. Acta* **2017**, *224*, 178−185.
(35) Zhu, S.; Hu, X.; Zhang, L.; Shao, M. Impacts of Perchloric Acid, Nafion, and Alkali Metal Ions on Oxygen Reduction Reaction Kinetics in Acidic and Alkaline Solutions. *J. Phys. Chem. C* **2016**, *120*, 27452−27461.
(36) Shinozaki, K.; Zack, J. W.; Pylypenko, S.; Pivovar, B. S.; Kocha, S. S. Oxygen Reduction Reaction Measurements on Platinum Electrocatalysts Utilizing Rotating Disk Electrode Technique II. Influence of Ink Formulation, Catalyst Layer Uniformity and Thickness. *J. Electrochem. Soc.* **2015**, *162*, F1384−F1396.
(37) Imai, H.; Izumi, K.; Matsumoto, M.; Kubo, Y.; Kato, K.; Imai, Y. In Situ and Real-Time Monitoring of Oxide Growth in a Few Monolayers at Surfaces of Platinum Nanoparticles in Aqueous Media. *J. Am. Chem. Soc.* **2009**, *131*, 6293−6300.
(38) Garrick, T. R.; Moylan, T. E.; Yarlagadda, V.; Kongkanand, A. Characterizing Electrolyte and Platinum Interface in PEM Fuel Cells Using CO Displacement. *J. Electrochem. Soc.* **2017**, *164*, F60−F64.
(39) Li, Y.; Intikhab, S.; Malkani, A.; Xu, B.; Snyder, J. Ionic Liquid Additives for the Mitigation of Nafion Specific Adsorption on Platinum. *ACS Catal.* **2020**, *10*, 7691−7698.
(40) Mansour, A. N.; Cook, J. W.; Sayers, D. E. Quantitative technique for the determination of the number of unoccupied d-electron states in a platinum catalyst using the L2,3 x-ray absorption edge spectra. *J. Phys. Chem.* **1984**, *88*, 2330−2334.

https://dx.doi.org/10.1021/acsaem.0c02326
ACS Appl. Energy Mater. 2021, 4, 1143−1149